CHEMBIOCHEM

DOI: 10.1002/cbic.200800834

Disulfide Bonds versus Trp···Trp Pairs in Irregular β-Hairpins: NMR Structure of Vammin Loop 3-Derived Peptides as a Case Study

Yasmina Mirassou,[a] Clara M. Santiveri,[a] M. Jesús Pérez de Vega,[b] Rosario González-Muñiz,[b] and M. Angeles Jiménez*[a]

Structural studies on model peptides have led to a good understanding of the rules behind the formation and stability of regular β-hairpins. To test their applicability to the successful design of irregular β-hairpins with long loops and/or β-bulges at the strands, we mimicked loop 3 of vammin, a 4:6 β-hairpin with a non-Gly β-bulge. The most stabilising cross-strand pairs, disulfide bonds or/and Trp···Trp pairs, were incorporated at non-hydrogen-bonded sites in peptides spanning the 69–80 region of vammin. According to NMR data, these modified peptides adopt β-hairpin conformations as intended by design. The Trp-containing peptides reproduce even the unusual positive ϕ angle for the Gln residue, with the indole rings in the preferred edge-to-face orientation. For the first time the β-hairpin-stabilising capacities of a disulfide bond and a Trp···Trp pair are compared in the same model system. We found that the contribution to stability of the noncovalent indole–indole interaction is larger than that of the covalent disulfide bond, and that their combination gives rise to an even more stable β-hairpin.

Introduction

As a result of the numerous studies on model β-hairpin peptides performed by several research groups in the last two decades,[1–12] nowadays a large amount of information exists on the factors contributing to β-hairpin formation and stability. Most of these studies were done in regular β-hairpins that have short loops with well-defined turn conformations (I′ and II′ in 2:2 hairpins, and I+G1 β-bulge in 3:5 hairpins[8–12]). β-Hairpin motifs are classified by using a X:Y nomenclature,[13] where X is the number of residues in the loop, and Y depends on whether the CO and NH groups of the two residues that precede and follow the loop, form two hydrogen bonds, Y = X, or only one, Y = X + 2. It is time to test if existent knowledge on β-hairpin formation can be applied successfully to the design of irregular β-hairpins, such as those whose strands contain β-bulges and/or with long loops that cannot be ascribed to canonical β turns. β-bulges are β-sheet irregularities, that is, regions where parallel or antiparallel hydrogen-bonded networks are disrupted, mainly as consequence of the insertion of extra residues. They are named as classic, wide, bent, G1 and special according to the number of residues involved and the hydrogen-bonding pattern.[14] As far as we know, the only irregular β-hairpin peptides that have been studied are those derived from the C-terminal 4:6 β-hairpin of protein G.[2,15] From a practical point of view, one interesting application of the current known "rules" for β-hairpin formation is the design of improved bio-active peptides that sometimes have irregular β-hairpin conformations. Given the essential role played by the turn in β-hairpin formation,[5,7,15–22] the easiest solution to stabilise β-hairpins with long loops would be to convert the loop regions into canonical turns. However, this is not always feasible because residues at the turn might be essential for activity; this occurs in some antimicrobial β-hairpin peptides[23,24] and in β-hairpin inhibitors of viral protein–RNA interactions.[25] The design of lead peptides that are able to inhibit therapeutically relevant protein–protein interactions, a field of great current interest, might consist in mimicking protein β-hairpins that are sometimes irregular.[26–30]

Blocking angiogenesis, a process crucial in tumour development and metastasis, constitutes a promising alternative strategy in cancer treatment. In this field, the interactions between the vascular endothelial growth factor (VEGF), a pro-angiogenic agent, and its specific membrane receptors, Flt-1 and KDR, constitute excellent targets in the search for new anti-angiogenic agents. Interestingly, mutagenesis studies on VEGF, whose structure has been solved in solution and in the crystalline state[31,32] indicate that a β-hairpin region, loop 3, is specifically involved in the interaction with the receptor KDR.[33,34] Furthermore, an N-to-C cyclic peptide encompassing loop 3 sequence was reported to have anti-angiogenic properties.[35] Interestingly, some members of the VEGF protein family, such as

[a] Y. Mirassou, Dr. C. M. Santiveri, Dr. M. A. Jiménez
Instituto de Química Física Rocasolano, CSIC
Serrano 119, 28006 Madrid (Spain)
Fax: (+34) 91-5642431
E-mail: majimenez@iqfr.csic.es

[b] Dr. M. J. Pérez de Vega, Dr. R. González-Muñiz
Instituto de Química Médica, CSIC
Juan de la Cierva 3, 28006 Madrid (Spain)

Supporting information for this article is available on the WWW under http://dx.doi.org/10.1002/cbic.200800834.

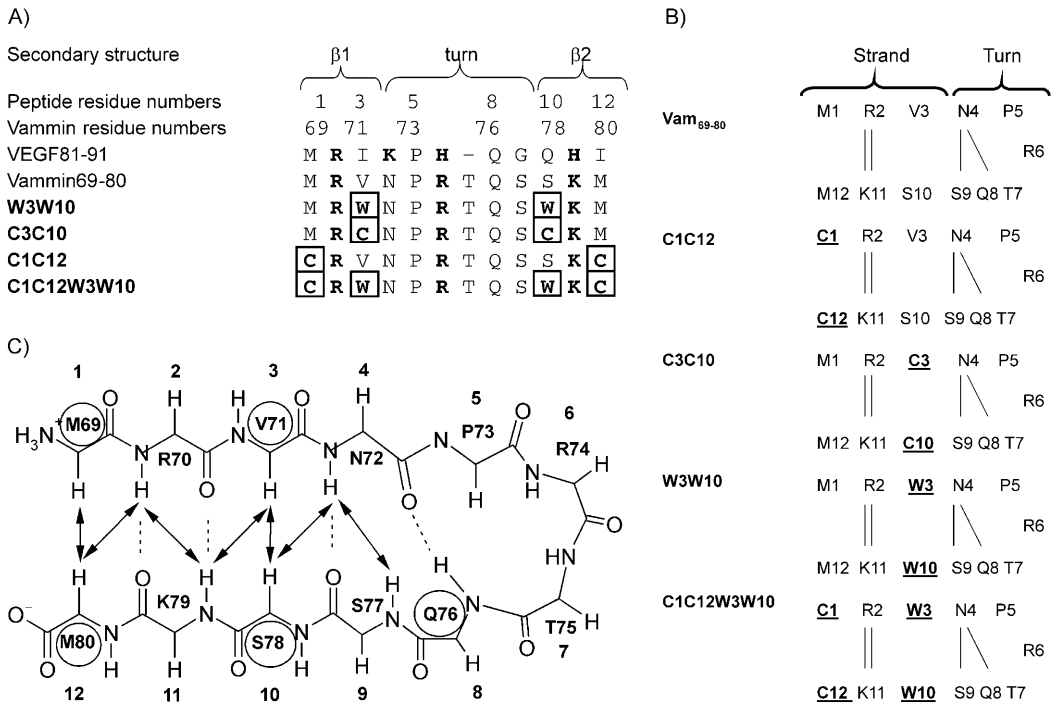

Figure 1. A) Sequence alignment of the loop 3 in VEGF (residues 81–91), the loop 3 in vammin (residues 69–80), and the vammin-derived peptides. Residue numbers for the intact vammin and for the 12-residue vammin-derived peptides are indicated. Turn and strand regions are indicated at the top. Positively charged residues are shown in bold and the Cys and Trp residues in bold and boxed. B) Peptide sequences. β-Sheet hydrogen bonds are shown by vertical lines. Turn and strand regions are indicated at the top. Cys and Trp residues are shown in bold and underlined. C) Schematic representation for backbone atoms of residues 69–80 of loop 3 in intact vammin (1WQ8). Residues whose side chains are oriented upward of the β-sheet plane are circled. Hydrogen bonds are shown as broken lines and expected NOEs involving backbone atoms as arrows. The residue numbers used in the 12-residue vammin-derived peptides are also indicated.

vammin, a VEGF isolated from snake venom, show high selectivity for KDR, and do not bind at all with Flt-1.[36] Moreover, the loop 3 structure in vammin is slightly different from that in VEGF-A,[36] in particular, it exhibits a one-residue insertion (Thr75; Figure 1). This extends the range of β-hairpins to be mimicked with the aim of finding inhibitors of the VEGF–KDR interaction. In this sense, we have addressed the design of 12-residue peptides derived from loop 3 in vammin, which is an antiparallel 4:6 β-hairpin showing a non-Gly β-bulge and overlapping β turns of type IV and I at the loop region (1WQ8,[36] Promotif analyses as reported in Pdbsum, http://www.ebi.ac.uk/pdbsum/).[37,38] To mimic this hairpin, residues that are considered to be important for KDR binding were conserved and either disulfide bonds,[39,40] or the favourable Trp···Trp pair residue,[41–44] or both were incorporated in the strands (Figure 1). The structural behaviour of these peptides in aqueous solution was examined by using NMR spectroscopy. A comparison of the ability of these peptides to adopt the wild-type β-hairpin structure constitutes an excellent case study to examine the rational design of irregular β-hairpins. Moreover, the relative contributions of disulfide bonds and Trp···Trp pairs to β-hairpin stability are analysed for the first time in the same peptide system.

Results

Peptide design

The criteria to design analogues of vammin loop 3 that are able to mimic the native irregular β-hairpin structure consisted in the incorporation of stabilising interactions at positions that are not essential for binding to KDR. Thus, positively charged residues R70 and R74, and the complete loop region (residues 72–77) were conserved in the designed derivatives (Figure 1). The importance of R70 and R74 is suggested by site-directed mutagenesis studies, which have revealed the involvement in the interaction with the KDR receptor of the equivalent residues R82 and H86 in VEGF (Figure 1[33,34]). As cross-strand-stabilising interactions, we selected those that are considered to be the best ones: disulfide bonds[39,40] and Trp···Trp pairs.[41–44] They were incorporated in the strands at the non-hydrogen-bonded sites (M69M80 and V71–S78; Figure 1). The peptides, **C1C12**, **C3C10**, **W3W10** and **C1C12W3W10** (Figure 1) were designed in a way that makes the comparison of the stabilising contributions of disulfide bonds and Trp···Trp pairs feasible, and to examine whether the two contributions are additive or not. The linear peptide encompassing residues 69–80 of vammin, denoted as $\mathbf{Vam_{69-80}}$ (Figure 1), was used as a control.

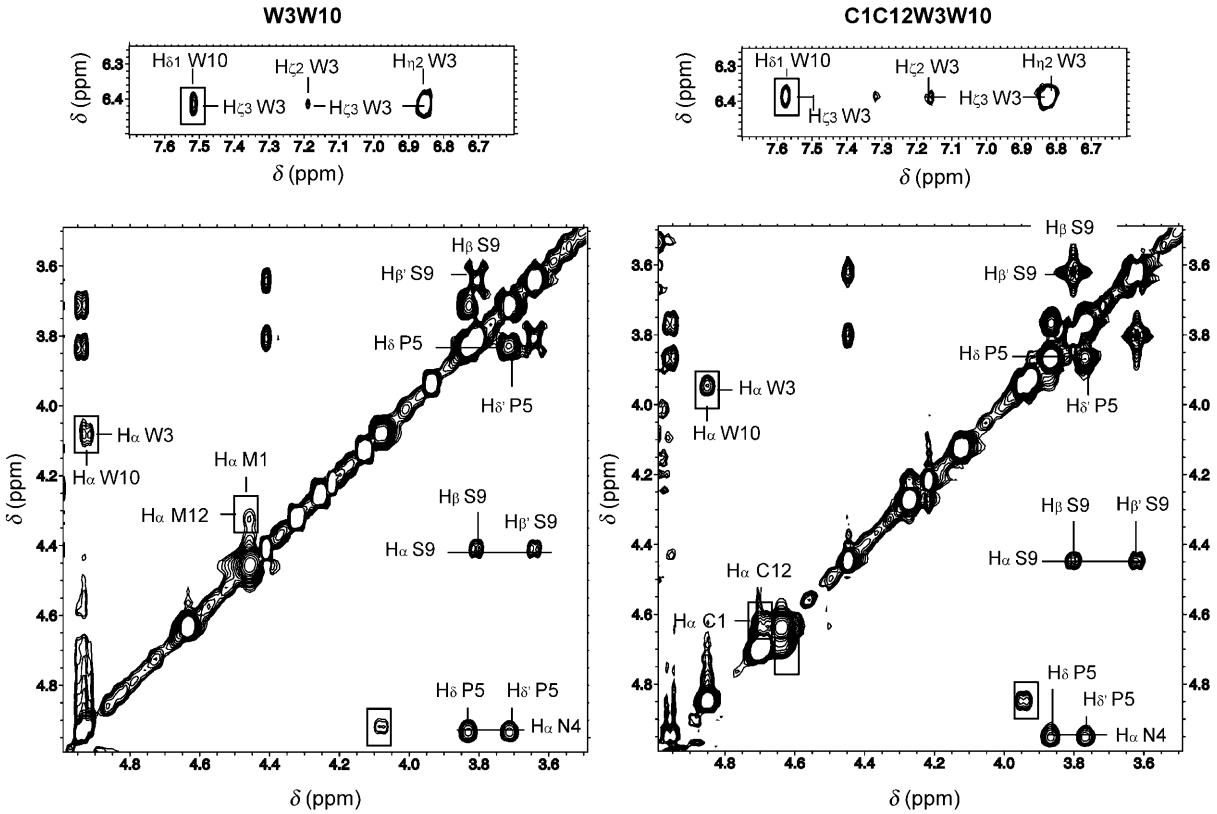

Figure 2. Selected NOESY spectral regions of peptides **W3W10** and **C1C12W3W10** in D_2O at pH 5.5 and 5 °C. NOEs are labelled on one side of the diagonal. In addition, long-range NOEs are boxed.

NMR spectroscopy conformational study

To assess whether the designed peptides are really able to adopt conformations similar to that of vammin loop 3, their structural behaviour was investigated in aqueous solution by analysis of several NMR spectroscopy parameters, NOE connectivities and ^1H and ^{13}C chemical shifts. As with most proline-containing peptides, the NMR spectra of all vammin-derived peptides displayed some minor signals that come from the *cis* conformation. That the major species is the *trans*-Pro rotamer was confirmed in all cases by the differences between the Pro $^{13}C_\beta$ and $^{13}C_\gamma$ chemical shifts ($\Delta\delta^{Pro} = \delta_{C\beta} - \delta_{C\gamma}$, ppm), which are in the 4.9–5.2 ppm range[45] and by the observation of the characteristic sequential NOEs between the H_α proton of N4 and the H_δ and $H_{\delta'}$ protons of P5 (Figure 2). From hereon, analysis of the NMR parameters refers to the major *trans* species.

The absence of nonsequential NOE connectivities and the closeness of $^1H_\alpha$, $^{13}C_\alpha$ and $^{13}C_\beta$ chemical shifts to their random coil values ($|\Delta\delta_{H\alpha}| < 0.1$ ppm, $|\Delta\delta_{C\alpha}| < 0.5$ ppm and $|\Delta\delta_{C\beta}| < 0.5$ ppm, except for N4, which exhibits the behavioural characteristics of Pro-preceding residues;[46] see Figure S1 in the Supporting Information), indicate that the linear peptide **Vam$_{69-80}$** in aqueous solution behaves as a mainly random-coil peptide. In contrast, the NMR parameters observed for all the other vammin-derived peptides, in particular, the presence of nonsequential NOEs that constitutes the strongest evidence for structure formation, are indicative of some ordered structures. More interestingly, the long-range NOEs of the backbone protons exhibited by the vammin analogues are the same as those that are expected for the strand alignment of vammin loop 3 (Figure 1C, Table 1). The number and intensity of these NOEs is especially remarkable in the case of peptides **W3W10** and **C1C12W3W10**. Some of the nonsequential NOEs observed for these two peptides are highlighted in the NOESY spectral region shown in Figure 2. Nonsequential NOEs that involve

Table 1. Intensities of the nonsequential NOEs involving backbone protons characteristic of the β-hairpin structure (see Figure 1) observed for vammin-derived peptides in aqueous solution at pH 5.5 and 5 °C.

^1H resonance in residue		NOE intensity[a] in peptide				X-ray distances
i	*j*	**C1C12**	**C3C10**	**W3W10**	**C1C12W3W10**	[Å]
H_α 1	H_α12	–	–	m[b]	s[b]	2.39
NH R2	NH K11	–	–	–	Ov.	2.94
NH R2	H_α 12	–	–	Ov.	Ov.	3.37
H_α 3	NH K11	Ov.	–	–	w	3.75
H_α 3	H_α 10	Ov	m[b]	s[b]	s[b]	2.45
NH N4	NH S9	–	–	–	m	3.53
NH N4	H_α 10	vw	–	Ov.	Ov.	3.66
H_α P5	NH Q8	–	–	w	m	4.00
H_α P5	H_α Q8	–	–	m[b]	m[b]	4.06

[a] NOE intensities are classified as strong (s), medium (m), weak (w) and very weak (vw). "Ov" refers to those NOE cross-peaks that can not be observed due to overlap with solvent signal, with other cross-peaks or closeness to diagonal. [b] Intensity from NOESY spectra recorded in D_2O.

side-chain protons observed for the designed peptides are also compatible with the structure of vammin loop 3 (Figure 1), for example, the NOEs between the side-chain protons of facing residues 3 and 10 observed for the peptides with Trp residues at these positions (Figure 1), and those between the methyl group of Thr7 and the amide side-chain protons of Asn4 seen for peptides **C1C12**, **W3W10** and **C1C12W3W10**. Strikingly, peptide **C3C10** exhibits NOEs involving the protons of the Asn4 and Gln8 side chains, which are pointing outwards on different sides of the β-sheet plane in native vammin loop 3 (Figure 1).

^{1}H and ^{13}C conformational shift values ($\Delta\delta = \delta^{observed} - \delta^{random\ coil}$, ppm) provide further confirmation that the four peptides adopt β-hairpin conformations. Thus, most residues exhibit conformational shifts that are large in absolute value and conform to the pattern expected for β-hairpins, that is, positive $\Delta\delta_{H\alpha}$, $\Delta\delta_{C\beta}$ and $\Delta\delta_{NH}$ and negative $\Delta\delta_{C\alpha}$ values at the strands, and some residues with the opposite sign at the turn region (Figure S1). Detailed analyses of chemical shift deviations at the loop region, residues 4–9, indicate that the two Trp-containing peptides are mimicking the features of loop 3 in native vammin, and that those of peptides **C1C12** and **C3C10**, particularly the last one, show some differences. The close similitude to vammin loop 3 is indicated by the fact that the $\Delta\delta_{H\alpha}$, $\Delta\delta_{C\alpha}$, $\Delta\delta_{C\beta}$ and $\Delta\delta_{NH}$ values of residues 4–9 in peptides **W3W10** and **C1C12W3W10** match with those expected for loop residues in 4:4/4:6 β-hairpins that have ϕ and ψ dihedral angles in the β-α_R-α_R-γ_R-γL-β regions of the Ramachandran map,[47–49] as do those occupied by the corresponding 72–77 residues in vammin (PDB ID: 1WQ8[36]). The negative $\Delta\delta_{H\alpha}$ value observed for S9 instead of the positive one expected for a β-sheet residue is the only exception, and it is explained by anisotropy effects from the close aromatic rings. It is particularly remarkable that the chemical shift deviations observed for Q8 in peptides **W3W10** and **C1C12W3W10** (Figure 3) are in agreement with its ϕ and ψ dihedral angles being in the γ_L region, as displayed by Q76 in vammin, but quite uncommon for non-Gly residues. The profiles of conformational shifts presented by peptides **C1C12** and **C3C10** differ from that are observed for the Trp-containing peptides (Figure S1). In particular, significant differences, that is, opposite signs, occur mainly for $\Delta\delta_{H\alpha}$ and $\Delta\delta_{C\beta}$ values of residue T7, and in the case of peptide **C3C10** also for the $\Delta\delta_{H\alpha}$, $\Delta\delta_{C\alpha}$ and $\Delta\delta_{C\beta}$ values of residue Q8 (Figure 3). This suggests that peptides **C1C12** and **C3C10** do not reproduce the loop 3 characteristics as well as peptides **W3W10** and **C1C12W3W10** do, as seen in the calculated structures (see below).

Chemical shifts for the aromatic rings of the two Trp residues present in peptides **W3W10** and **C1C12W3W10** merit further consideration because they provide information about their relative orientation.[44] In peptides **W3W10** and **C1C12-W3W10**, the chemical shifts of the $H_{\varepsilon 3}$ and $H_{\beta\beta'}$ protons of W3 are considerably up-field shifted (Table S1), which is a characteristic of Trp indole rings in an edge disposition. Thus, the aromatic ring of W3 probably adopts an edge orientation relative to that of W10, as is found in the calculated structures (see below).

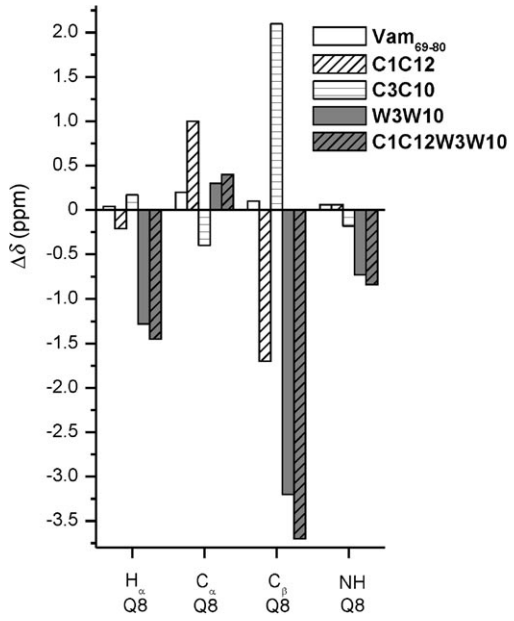

Figure 3. Histograms showing the $\Delta\delta_{H\alpha}$ ($\Delta\delta_{H\alpha} = \delta_{H\alpha}^{observed} - \delta_{H\alpha}^{random\ coil}$, ppm), $\Delta\delta_{C\alpha}$ ($\Delta\delta_{C\alpha} = \delta_{C\alpha}^{observed} - \delta_{C\alpha}^{random\ coil}$, ppm), $\Delta\delta_{C\beta}$ ($\Delta\delta_{C\beta} = \delta_{C\beta}^{observed} - \delta_{C\beta}^{random\ coil}$, ppm) and $\Delta\delta_{NH}$ ($\Delta\delta_{NH} = \delta_{NH}^{observed} - \delta_{NH}^{random\ coil}$, ppm) values exhibited by residue Q8 in peptides **Vam$_{69-80}$** (white bars), **C1C12** (tilted stripped bars), **C3C10** (horizontal stripped bars), **W3W10** (grey bars) and **C1C12W3W10** (grey tilted stripped bars) in aqueous solution at pH 5.5 and 5 °C. Random coil values for the ^{1}H chemical shifts of H_α protons and for the ^{13}C chemical shifts of C_α and C_β carbons were taken from Wishart et al., 1995.[46] $\Delta\delta_{NH}$ values were obtained by using the CSDb program[15,49,74]

To visualise and get further insights into the preferred conformations adopted by the designed peptides, we performed structure calculations on the basis of distance restraints derived from the observed nonsequential NOEs and dihedral angle constraints obtained from the $^{1}H_\alpha$, $^{13}C_\alpha$ and $^{13}C_\beta$ chemical shifts (see the Experimental Section). The structures calculated for the designed peptides are well defined, in particular those of the two Trp-containing peptides (see Figure 4 and the low RMSD values reported in Table S2). It is noticeable that the relative orientation of the two indole rings is also well defined (Figure 4), as expected by the numerous NOE correlations involving the side-chain protons of the two Trp residues that were observed in the NOESY spectra of **W3W10** and **C1C12-W3W10** (Figure 2). The two indole rings are in an edge-to-face orientation in which the W3 occupies the edge position and the W10 the face one, as has been deduced from chemical shift analyses (see above).

CD spectra of Trp-containing peptides

The far-UV CD spectra of peptides **W3W10** and **C1C12W3W10** (Figure 5 A) display a positive band at ~191 nm and a negative band at 215 nm, which are both characteristic of a β-sheet structure.[50] We can also observe an intense positive band at 228 nm that corresponds to a large exciton couplet that is attributable to the interaction between the aromatic chromophores.[44,51,52] All bands are more intense in peptide **C1C12-W3W10** than in peptide **W3W10**. This indicates that the folded

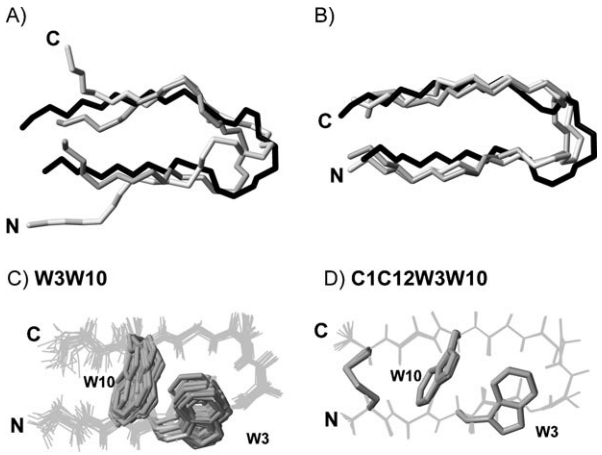

Figure 4. Peptide structures. Top: Superposition of the backbone atoms for the lowest target function structure calculated for: A) peptides **C1C12** (grey), **C3C10** (white) and region 69–80 of vammin (black, 1WQ8[36]), and B) peptides **C1C12W3W10** (grey), **W3W10** (white) and region 69–80 of vammin (black; 1WQ8;[36]). Bottom: Superposition of the 20 lowest target function structures calculated for peptides C) **W3W10** and D) **C1C12W3W10**. Backbones are shown as grey lines and side chains for Trp and Cys residues are highlighted in grey neon. N- and C-ends are labelled in the four panels.

structure is more populated in **C1C12W3W10** than in **W3W10**, in agreement with the NMR data (see below).

Non-zero near-UV CD spectra of peptides containing aromatic residues are indicative of the aromatic rings adopting some ordered structures, but interpretation of the observed bands is hampered by the fact that aromatic rings have positive and negative contributions in the near-UV CD spectrum.[53] Peptides **W3W10** and **C1C12W3W10** (Figure 5 B) exhibit a similar near-UV CD spectra, with two negative bands at 286 and 294 nm and a positive band at 288 nm; only the intensity of the bands, which is slightly stronger in peptide **C1C12W3W10**, is different. This indicates that the side chains of the two aromatic tryptophan residues present in both peptides (W3 and W10) adopt the same geometry and have a similar environment, as confirmed in the structures calculated from the NMR constraints (Figure 4). The intensity differences are in concordance with the folded structure of peptide **C1C12W3W10** being more populated than that of peptide **W3W10**, as deduced from far-UV CD spectra and from the NMR parameters (see next section).

Ranking of β-hairpin populations

To compare the stabilisation effects of Trp···Trp pairs and disulfide bonds it is necessary to order the peptides according to their β-hairpin populations. Because of the unreliability of references for the 100% and 0% β-hairpin populations the absolute populations obtained from the chemical-shift-based methods that have been proposed to quantify β-hairpin populations[48,49,54–58] can only be considered as estimates, but the qualitative rankings that come from them are reliable. Therefore, we ranked the ability of the peptides to adopt β-hairpin structures in a qualitative way. To minimise the influence of the anisotropy effects caused by aromatic ring currents (the two Trp residues present in peptides **W3W10** and **C1C12W3W10**; Figure 1) and also considering that the sequence differences in this set of peptides are at the strands (Figure 1), we selected chemical shifts from residues at the turn region that are greatly affected upon β-hairpin formation as the best probes to order the vammin-derived peptides. These selected probes are: the difference in ^{1}H chemical shift between the two H_β protons of N4 ($\Delta\delta_{\beta\beta'}^{N4}$), the ^{1}H chemical shift deviations for the NH amide and H_α protons of R6 ($\Delta\delta_{NH}^{R6}$ and $\Delta\delta_{H\alpha}^{R6}$), the ^{13}C chemical shift deviations for the $^{13}C_\alpha$ and $^{13}C_\beta$ carbons of R6 ($\Delta\delta_{C\alpha}^{R6}$ and $\Delta\delta_{C\beta}^{R6}$) and the ^{1}H chemical shift deviations for the NH amide and methyl group of T7 ($\Delta\delta_{NH}^{T7}$ and $\Delta\delta_{H\gamma}^{T7}$). According to them (Figure 6), β-hairpin populations follow the decreasing order: **C1C12W3W10** > **W3W10** ≫ **C3C10** > **C1C12** ≫ **Vam$_{69-80}$** (random coil).

Discussion

β-Hairpin designed peptides versus native vammin loop 3

According to the NMR data, **Vam$_{69-80}$**, the 12-residue peptide encompassing the native sequence of vammin loop 3, is mainly random coil. The design of peptides derived from that sequence by incorporation of stabilising pair interactions was successful, because the four designed peptides adopt β-hairpin structures as evidenced from the analysis of NMR data (see above); but are the structural features of the irregular loop of vammin maintained in the designed peptides? To respond to this question, the structures calculated for the four peptides were compared with that of loop 3 in the crystal structure of vammin (1WQ8,[36] Figure 4 and Table S2).

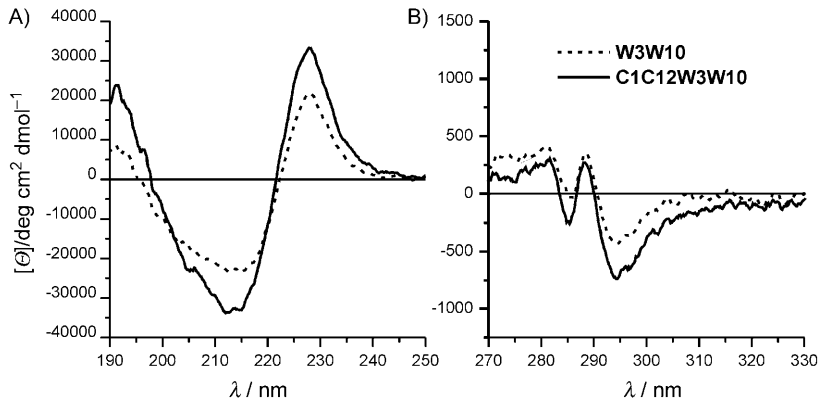

Figure 5. A) Far-UV and B) near-UV CD spectra of peptides **W3W10** (broken line) and **C1C12W3W10** (continuous line) in aqueous solution at pH 5.5 and 5 °C.

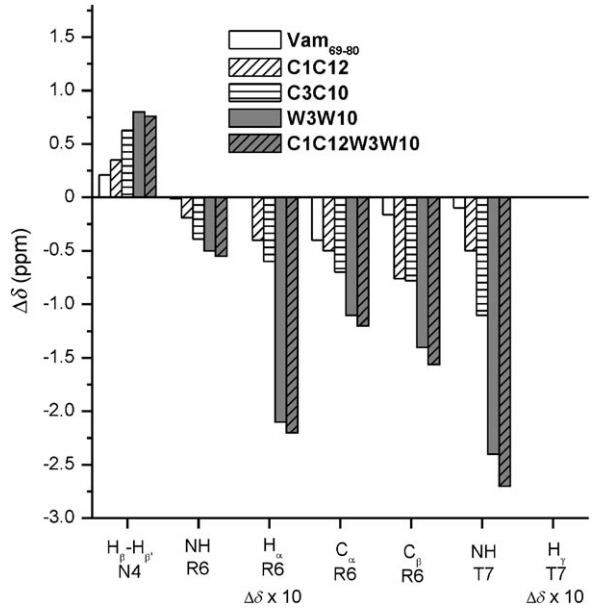

Figure 6. Histograms showing chemical shift deviations representative as probes for β-hairpin populations shown by peptides **Vam$_{69-80}$** (white bars), **C1C12** (tilted stripped bars), **C3C10** (horizontal stripped bars), **W3W10** (grey bars), and **C1C12W3W10** (grey tilted stripped bars) in aqueous solution at pH 5.5 and 5 °C. Random coil values for the selected ^{1}H and ^{13}C chemical shifts were taken from Wishart et al., 1995[46] with the exception of $\Delta\delta_{NH}$ values that were obtained by using the CSDb program.[15,49,74] Values for H_α and H_γ protons belonging to R6 and T7, respectively, are multiplied by 10 in the plot.

Based on the RMSD values displayed by the structures adopted by the peptides relative to that of native vammin loop 3 and the twist angles between the two β-strands (Figure 4 and Table S2), peptides **C1C12**, **W3W10** and **C1C12W3W10** adopt a β-hairpin quite similar to that of vammin loop 3, while the one formed by peptide **C3C10** differed appreciably. This is in agreement with the profiles of conformational shifts ($\Delta\delta$) for peptide **C3C10** exhibiting significant differences relative to the other peptides (Figures 3 and S1). In particular, it is remarkable that peptides **W3W10** and **C1C12W3W10** exhibit an unusually positive ϕ angle for residue Gln8, as occurs in native vammin (Table S2). It seems that the side-chain packing between the two Trp residues at the non-hydrogen-bonded site closest to the turn helps to fit the native vammin loop conformation more efficiently than a disulfide bond placed at the same position (Figure 1). It looks plausible that Trp···Trp pairs are a better choice than disulfide bonds to fit irregular β-hairpin loops. The two Trp-containing peptides also exhibit structural features different from native vammin. The main difference consists of a tighter side-chain packing in the β-sheet face where the Trp···Trp pair is located, which is also the most hydrophobic face (Figures 1, 4 and S2). This tighter side-chain packing also involves the Gln side chain and seems to slightly fold the loop region up and away from the β-sheet plane, while the β-sheet and loop backbones look more coplanar in native vammin.

Disulfide bonds versus Trp···Trp pairs in β-hairpin stability

Independent of their capacity to mimic loop 3 of vammin, the sequences of the designed peptides (Figure 1; excluding the linear wild-type peptide) are useful for comparing the contributions of disulfide bonds and Trp···Trp pairs to β-hairpin stability. In addition, we can analyse whether their contributions are compatible and/or additive, and get insights into the geometry of the interacting Trp···Trp side chains.

First, we examine peptides **C3C10** and **W3W10**, whose sequences differ in a single cross-strand side chain–side chain interaction (Figure 1). Hence, differences in their conformational behaviour will give us clues about the relative stabilising capacities of a disulfide bond and a Trp···Trp pair. The β-hairpin population adopted by peptide **W3W10** is clearly larger than that adopted by peptide **C3C10** (Figure 6). This result fully agrees with previous works that used different β-hairpin peptide models to estimate the stabilising contribution of a Cys–Cys pair in a non-hydrogen-bonded position as about 1.0 kcal mol^{-1},[58] and that of Trp···Trp pairs as about 1.2 kcal mol^{-1}.[41,59] The Trp···Trp pair contribution has also been quantified by using a small three-stranded antiparallel β-sheet protein instead of the simpler β-hairpin models. The smaller contribution of the Trp···Trp pair found in this case (0.6 kcal mol^{-1} [43]) might come from context effects on the Trp···Trp interaction. Apart from the stability differences, incorporation of a disulfide bond in the vammin peptide system results in a β-hairpin structure with some topological features distinct from those displayed by the peptide containing the Trp···Trp pair. Thus, in the structures calculated from the distance and angle restraints derived from the experimental NMR parameters, the strands in the β-hairpin formed by peptide **C3C10** diverge at their N and C-terminal ends (Figure 4 and Figure S2). In contrast, the side chains of the N- and C-terminal Met residues in peptide **W3W10** are close and interact with the indole ring of Trp10 (Figure 4 and Figure S2). In brief, our results suggest that to stabilise β-hairpin structures is better to incorporate a Trp···Trp pair than a disulfide bond. Although the stabilising ability of the Trp···Trp pair had been previously recognised and successfully applied,[41,52,59,60] as far as we know, this is the first time that its stabilising capacity is directly compared to that of a disulfide bond.

It is also interesting to analyse whether disulfide bond and Trp···Trp pair contributions sum up to increase the β-hairpin stability. To this aim, we compared β-hairpin formation in peptide **C1C12W3W10** relative to peptides **C1C12** and **W3W10** (Figure 1). As expected, the most populated β-hairpin was that formed by peptide **C1C12W3W10** (Figure 6) which indicates that disulfide bonds and Trp···Trp pairs are compatible and additive. In this sense, it is interesting to note that the disulfide bond and the indole rings hardly contact one another in the structure calculated for peptide **C1C12W3W10** (Figure 4). This suggests that the favourable contributions to stability of the disulfide bond and the Trp···Trp are independent and then probably additive, though their compatibility probably depends on their relative positions within the β-hairpin.

Geometry of the interacting Trp···Trp side chains

Interacting Trp···Trp pairs can adopt different orientations, edge-to-face, parallel-displaced and face-to-face; edge-to-face is the most frequent geometry found in statistical surveys on protein structures[61,62] and the one that is favoured according to quantum mechanical calculations.[63] The large preference for the edge-to-face geometry seems to be mainly due to an electrostatic multipole interaction between the Trp side chains and not to classical hydrophobic interaction.[63] Two different edge-to-face geometries can be distinguished in the case of Trp···Trp residues facing each other in antiparallel β sheets, the edge-to-face and the face-to-edge[52] depending on whether the edge Trp is located at the N-terminal or at the C-terminal β strand, respectively. Both orientations have been found in β-hairpins containing Trp···Trp pairs,[42,44,52,59,60,64]

In this scenario, according to chemical shift and NOE data (see Results), the aromatic rings of the Trp···Trp pairs present in peptides **W3W10** and **C1C12W3W10** adopt edge-to-face orientations (Figure 4). The presence of a disulfide bond in peptide **C1C12W3W10** increases the β-hairpin stability, but the interaction between the indole rings remains unaffected. In fact, chemical shifts for the $H_{\beta\beta'}$ protons of the two Cys residues linked by the disulfide bond are not up-field (see Table S1), unlike those in a β-hairpin peptide that contains a Trp···Ile pair in a position relative to the disulfide bond equivalent to that of the Trp···Trp pair in peptide **C1C12W3W10**.[58] In agreement with this, the disulfide bond and the indole rings hardly interact in the structure calculated for peptide **C1C12W3W10** (Figure 4).

Conclusions

A 12-residue peptide encompassing the sequence of an irregular 4:6 β-hairpin in the native structure of vammin behaves as a mainly random-coil peptide. To mimic this vammin β-hairpin, designated loop 3, disulfide bonds or/and Trp···Trp pairs, which are known to be the most stabilising cross-strand pair interactions in β-hairpins[41–44,65] were incorporated at non-hydrogen-bonded sites. The NMR data for the four vammin-derived peptides support the idea that all of them adopt β-hairpin conformations, as intended by design. The similitude to the native loop 3 of vammin is particularly remarkable in the case of the Trp-containing peptides that reproduce the unusual positive ϕ angle for the Gln residue at the turn region. Since the design criteria come from the existing knowledge on β-hairpin formation and stability that is derived mainly from studies on regular 2:2 and 3:5 β-hairpins with short loops, the success in the loop 3-mimicking ability of the designed peptides demonstrates the validity of that knowledge to β-hairpins with longer loops such as the vammin 4:6 β-hairpin. In this system, the indole rings of the Trp···Trp pair adopt an edge-to-face orientation that is preferred according to statistical analyses and molecular dynamic simulations.

More interestingly, we have found that the contribution to stability of a Trp···Trp cross-strand pair can be larger than that of a disulfide bond. As far as we know, this is the first time that the stabilising capacities of a disulfide bond and a Trp···Trp pair have been compared within the same peptide system. Furthermore, we have found that a disulfide bond plus a Trp···Trp pair together give rise to higher stability than each by itself.

Experimental Section

Peptide synthesis: Peptides were synthesised in the solid phase by using Fmoc (fluorenyl-9-methyloxycarbonyl) protocols and purified by reversed-phase HPLC (RP-HPLC) up to more than 95% purity by either NeoMPS (Strasbourg, France) or CASLO Laboratory ApS (Lyngby, Denmark).

Vam_{69-80}: RP-HPLC: $t_R = 12.8$ min; 97.2% (linear 10–60% A gradient for 25 min, A) 0.1% TFA in CH_3CN, B) 0.1% TFA in H_2O); HRMS: *m/z* calcd for $C_{57}H_{103}N_{21}O_{18}S_2$: 1434.7 $[M+H]^+$; found: 1434.5.

C1C12: RP-HPLC: $t_R = 12.7$ min; 99% (linear 0–30% A gradient for 30 min, A) 0.05% TFA in H_2O/CH_3CN (98:2); B) 0.05% TFA in H_2O/CH_3CN (1:9)). HRMS: *m/z* calcd for $C_{53}H_{93}N_{21}O_{18}S_2$: 1375.6 $[M+H]^+$; found: 1375.2.

C3C10: RP-HPLC: $t_R = 12.9$ min; 98.9% (linear 10–60% A gradient for 25 min, A) 0.1% TFA in CH_3CN, B) 0.1% TFA in H_2O); HRMS: *m/z* calcd for $C_{55}H_{97}N_{21}O_{17}S_4$: 1452.7 $[M+H]^+$; found: 1452.0.

W3W10: RP-HPLC: $t_R = 14.8$ min; 98% purity (linear 10–40% A gradient for 30 min, A) 0.05% TFA in H_2O/CH_3CN (1:9); B) 0.05% TFA in H_2O/CH_3CN (98:2)); HRMS: calcd *m/z* for $C_{71}H_{109}N_{23}O_{17}S_2$: 1619.8 $[M+H]^+$; found: 1619.4.

C1C12W3W10: RP-HPLC: $t_R = 15.0$ min; 98% (linear 10–60% A gradient for 25 min. A) 0.1% TFA in CH_3CN, B) 0.1% TFA in H_2O; HRMS: *m/z* calcd for $C_{67}H_{99}N_{23}O_{17}S_2$: 1562.8 $[M+H]^+$; found: 1562.1.

NMR spectra: NMR spectroscopic samples were prepared by dissolving the lyophilised peptide (~1 mg) in H_2O/D_2O (9:1 *v/v*, 0.5 mL) or in pure D_2O (0.5 mL). Peptide concentrations were about 1–2 mM. The pH was adjusted to 5.5 by adding minimal amounts of NaOD or DCl, measured with a glass microelectrode and not corrected for isotope effects. The temperature of the NMR spectroscopic probe was calibrated by using a methanol sample. Sodium 2,2-dimethyl-2-silapentane-5-sulfonate (DSS) was used as an internal reference. The ^1H NMR spectra were acquired on a Bruker Avance 600 spectrometer operating at a proton frequency of 600.13 MHz and equipped with a cryoprobe. 1D spectra were acquired by using 32 K data points, which were zero-filled to 64 K data points before performing the Fourier transformation. As previously reported,[20] phase-sensitive two-dimensional correlated spectroscopy (COSY), total correlated spectroscopy (TOCSY), and nuclear Overhauser enhancement spectroscopy (NOESY) spectra were recorded by using standard techniques by using presaturation of the water signal and the time-proportional phase incrementation mode. NOESY mixing times were 150 ms, and TOCSY spectra were recorded by using 60 ms DIPSI2 with z filter spin-lock sequence. The $^1H,^{13}C$ heteronuclear single quantum coherence spectra (HSQC) at natural ^{13}C abundance were recorded in 1–2 mM peptide samples in D_2O. Acquisition data matrices were defined by 2018 × 512 points in t_2 and t_1, respectively. Data were processed by using the TOPSPIN program.[66] The 2D data matrix was multiplied by either a square-sine-bell or a sine-bell window function, and the corresponding shift was optimised for every spectrum and zero-filled to a 2 K × 1 K complex matrix prior to Fourier transformation. Baseline correction was applied in both dimensions. The 0 ppm ^{13}C

δ-value was obtained indirectly by multiplying the spectrometer frequency that corresponds to 0 ppm in the ^{1}H spectrum, assigned to internal DSS reference, by 0.25144953.[67]

NMR spectroscopy assignment: Standard sequential assignment methods[68,69] were applied to assign the ^{1}H NMR signals of the vammin-derived peptides. Then, the ^{13}C resonances were straightforwardly assigned on the basis of the cross-correlations that were observed in the HSQC spectra between the proton and the bound carbon. The ^{1}H and ^{13}C δ-values are available as Supporting Information (Table S1).

Structure calculation: Distance constraints for structure calculations were derived from the 2D 150-ms-mixing-time NOESY spectra recorded either in H_2O or in D_2O. The NOE cross-peaks were integrated by using the automatic integration subroutine of the SPARKY program[70] and then calibrated and converted to upper-limit distance constraints within the CYANA program.[71] The ϕ and ψ angle restraints were derived from $^1H_\alpha$, $^{13}C_\alpha$ and $^{13}C_\beta$ chemical shifts by using the TALOS program.[72] The ϕ angles for those residues for which the derived angle restraints were ambiguous were constrained to the range -180° to 0°, except for Asn and Gly residues that, in proteins, sometimes exhibit positive ϕ angles. Structures were calculated by using the CYANA program[71] and an annealing strategy.

Structure analysis: Structures calculated for the cyclic peptides as well as that reported for vammin (PDB ID: 1WQ8) were examined by using the program MOLMOL.[73]

Circular Dichroism measurements: CD spectra were recorded in a Jasco J-810 spectropolarimeter equipped with a Peltier temperature control unit. The peptide samples (about 30 μM) were prepared in pure H_2O at pH 5.5. Far-UV and near-UV spectra were carried out by using cells with 0.1 cm and 1 cm path lengths, respectively. Experiments were recorded at 5 °C with a scan speed of 50 nm min^{-1}, a response time of 2 s, and 1 nm bandwidth. Spectra are the average of eight scans and were corrected by subtracting the baseline recorded for the solvent under the same conditions. Mean residue ellipticities, $[\Theta]$, are expressed in deg cm^2 dmol^{-1} according to the relationship $[\Theta]=\Theta/(10\,lcN)$, where Θ is the observed ellipticity, l is the cell path length in cm, c is the molar concentration of the peptide sample and N is the number of the amino acids in the sequence.

Acknowledgements

We thank financial support from CSIC Intramural projects 200580F0161 and 200580F0162 and from MICINN projects CTQ2008-00080/BQU and SAF2006-01205. C.M.S. acknowledges the CSIC I3P program for financial support from the European Social Fund.

Keywords: beta hairpin · circular dichroism · disulfide bonds · NMR spectroscopy · peptides · Trp–Trp interactions

[1] F. J. Blanco, M. A. Jiménez, J. Herranz, M. Rico, J. Santoro, J. L. Nieto, *J. Am. Chem. Soc.* **1993**, *115*, 5887–5888.
[2] F. J. Blanco, G. Rivas, L. Serrano, *Nat. Struct. Biol.* **1994**, *1*, 584–590.
[3] T. S. Haque, J. C. Little, S. H. Gellman, *J. Am. Chem. Soc.* **1994**, *116*, 4105–4106.
[4] E. deAlba, F. J. Blanco, M. A. Jiménez, M. Rico, J. L. Nieto, *Eur. J. Biochem.* **1995**, *233*, 283–292.
[5] M. S. Searle, D. H. Williams, L. C. Packman, *Nat. Struct. Biol.* **1995**, *2*, 999–1006.
[6] M. Ramírez-Alvarado, F. J. Blanco, L. Serrano, *Nat. Struct. Biol.* **1996**, *3*, 604–612.
[7] E. de Alba, M. A. Jiménez, M. Rico, *J. Am. Chem. Soc.* **1997**, *119*, 175–183.
[8] S. H. Gellman, *Curr. Opin. Chem. Biol.* **1998**, *2*, 717–725.
[9] E. Lacroix, T. Kortemme, M. Lopez de La Paz, L. Serrano, *Curr. Opin. Struct. Biol.* **1999**, *9*, 487–493.
[10] M. S. Searle, B. Ciani, *Curr. Opin. Struct. Biol.* **2004**, *14*, 458–464.
[11] R. M. Hughes, M. L. Waters, *Curr. Opin. Struct. Biol.* **2006**, *16*, 514–524.
[12] D. Pantoja-Uceda, C. M. Santiveri, M. A. Jiménez, *Methods Mol. Biol.* **2006**, *340*, 27–51.
[13] B. L. Sibanda, T. L. Blundell, J. M. Thornton, *J. Mol. Biol.* **1989**, *206*, 759–777.
[14] A. W. Chan, E. G. Hutchinson, D. Harris, J. M. Thornton, *Protein Sci.* **1993**, *2*, 1574–1590.
[15] R. M. Fesinmeyer, F. M. Hudson, N. H. Andersen, *J. Am. Chem. Soc.* **2004**, *126*, 7238–7243.
[16] T. S. Haque, S. H. Gellman, *J. Am. Chem. Soc.* **1997**, *119*, 2303–2304.
[17] M. Ramírez-Alvarado, F. J. Blanco, H. Niemann, L. Serrano, *J. Mol. Biol.* **1997**, *273*, 898–912.
[18] A. G. Cochran, R. T. Tong, M. A. Starovasnik, E. J. Park, R. S. McDowell, J. E. Theaker, N. J. Skelton, *J. Am. Chem. Soc.* **2001**, *123*, 625–632.
[19] C. M. Santiveri, J. Santoro, M. Rico, M. A. Jiménez, *J. Am. Chem. Soc.* **2002**, *124*, 14903–14909.
[20] C. M. Santiveri, D. Pantoja-Uceda, M. Rico, M. A. Jiménez, *Biopolymers* **2005**, *79*, 150–162.
[21] R. Rai, S. Raghothama, R. Sridharan, P. Balaram, *Biopolymers* **2007**, *88*, 350–361.
[22] M. Bonomi, D. Branduardi, F. L. Gervasio, M. Parrinello, *J. Am. Chem. Soc.* **2008**, *130*, 13938–13944.
[23] J. R. Lai, B. R. Huck, B. Weisblum, S. H. Gellman, *Biochemistry* **2002**, *41*, 12835–12842.
[24] J. Chen, T. J. Falla, H. Liu, M. A. Hurst, C. A. Fujii, D. A. Mosca, J. R. Embree, D. J. Loury, P. A. Radel, C. C. Chang, L. Gu, J. C. Fiddes, *Biopolymers* **2000**, *55*, 88–98.
[25] Z. Athanassiou, K. Patora, R. L. Dias, K. Moehle, J. A. Robinson, G. Varani, *Biochemistry* **2007**, *46*, 741–751.
[26] T. R. Gadek, *Biotechniques* **2003**, 21–24.
[27] L. Pagliaro, J. Felding, K. Audouze, S. J. Nielsen, R. B. Terry, C. Krog-Jensen, S. Butcher, *Curr. Opin. Chem. Biol.* **2004**, *8*, 442–449.
[28] L. O. Sillerud, R. S. Larson, *Curr. Protein Pept. Sci.* **2005**, *6*, 151–169.
[29] J. K. Murray, S. H. Gellman, *Biopolymers* **2007**, *88*, 657–686.
[30] J. A. Robinson, *Acc. Chem. Res.* **2008**, *41*, 1278–1288.
[31] C. Wiesmann, G. Fuh, H. W. Christinger, C. Eigenbrot, J. A. Wells, A. M. de Vos, *Cell* **1997**, *91*, 695–704.
[32] B. Pan, B. Li, S. J. Russell, J. Y. Tom, A. G. Cochran, W. J. Fairbrother, *J. Mol. Biol.* **2002**, *316*, 769–787.
[33] B. A. Keyt, H. V. Nguyen, L. T. Berleau, C. M. Duarte, J. Park, H. Chen, N. Ferrara, *J. Biol. Chem.* **1996**, *271*, 5638–5646.
[34] Y. A. Muller, B. Li, H. W. Christinger, J. A. Wells, B. C. Cunningham, A. M. de Vos, *Proc. Natl. Acad. Sci. USA* **1997**, *94*, 7192–7197.
[35] L. Zilberberg, S. Shinkaruk, O. Lequin, B. Rousseau, M. Hagedorn, F. Costa, D. Caronzolo, M. Balke, X. Canron, O. Convert, G. Lain, K. Gionnet, M. Goncalves, M. Bayle, L. Bello, G. Chassaing, G. Deleris, A. Bikfalvi, *J. Biol. Chem.* **2003**, *278*, 35564–35573.
[36] K. Suto, Y. Yamazaki, T. Morita, H. Mizuno, *J. Biol. Chem.* **2005**, *280*, 2126–2131.
[37] E. G. Hutchinson, J. M. Thornton, *Protein Sci.* **1996**, *5*, 212–220.
[38] R. A. Laskowski, *Nucleic Acids Res.* **2001**, *29*, 221–222.
[39] S. F. Betz, *Protein Sci.* **1993**, *2*, 1551–1558.
[40] K. Uma, R. Kishore, P. Balaram, *Biopolymers* **1993**, *33*, 865–871.
[41] S. J. Russell, A. G. Cochran, *J. Am. Chem. Soc.* **2000**, *122*, 12600–12601.
[42] A. G. Cochran, N. J. Skelton, M. A. Starovasnik, *Proc. Natl. Acad. Sci. USA* **2001**, *98*, 5578–5583.
[43] M. Jager, M. Dendle, A. A. Fuller, J. W. Kelly, *Protein Sci.* **2007**, *16*, 2306–2313.
[44] L. Eidenschink, B. L. Kier, K. N. Huggins, N. H. Andersen, *Proteins* **2008**; DOI: 10.1002/prot.22240.
[45] M. Schubert, D. Labudde, H. Oschkinat, P. Schmieder, *J. Biomol. NMR* **2002**, *24*, 149–154.

[46] D. S. Wishart, C. G. Bigam, A. Holm, R. S. Hodges, B. D. Sykes, *J. Biomol. NMR* **1995**, *5*, 67–81.
[47] J. M. Thornton, B. L. Sibanda, M. S. Edwards, D. J. Barlow, *Bioessays* **1988**, *8*, 63–69.
[48] C. M. Santiveri, M. Rico, M. A. Jimenez, *J. Biomol. NMR* **2001**, *19*, 331–345.
[49] R. M. Fesinmeyer, F. M. Hudson, K. A. Olsen, G. W. White, A. Euser, N. H. Andersen, *J. Biomol. NMR* **2005**, *33*, 213–231.
[50] S. Y. Venyaminov, J. T. Yang in *Circular Dichroism and the Conformational Analysis of Biomolecules* (Ed.: G. D. Fasman), Plenum, New York, **1996**, pp. 69–107.
[51] R. W. Woody, A. K. Dunker in *Circular Dichroism and the Conformational Analysis of Biomolecules* (Ed.: G. D. Fasman), Plenum, New York, **1996**, pp. 109–157.
[52] B. L. Kier, N. H. Andersen, *J. Am. Chem. Soc.* **2008**, *130*, 14675–14683.
[53] E. H. Strickland, *CRC Crit. Rev. Biochem.* **1974**, *2*, 113–175.
[54] A. J. Maynard, G. J. Sharman, M. S. Searle, *J. Am. Chem. Soc.* **1998**, *120*, 1996–2007.
[55] S. R. Griffiths-Jones, M. S. Searle, *J. Am. Chem. Soc.* **2000**, *122*, 8350–8356.
[56] J. F. Espinosa, F. A. Syud, S. H. Gellman, *Protein Sci.* **2002**, *11*, 1492–1505.
[57] C. D. Tatko, M. L. Waters, *J. Am. Chem. Soc.* **2002**, *124*, 9372–9373.
[58] C. M. Santiveri, E. León, M. Rico, M. A. Jiménez, *Chem. Eur. J.* **2008**, *14*, 488–499.
[59] N. H. Andersen, K. A. Olsen, R. M. Fesinmeyer, X. Tan, F. M. Hudson, L. A. Eidenschink, S. R. Farazi, *J. Am. Chem. Soc.* **2006**, *128*, 6101–6110.
[60] M. Favre, K. Moehle, L. Jiang, B. Pfeiffer, J. A. Robinson, *J. Am. Chem. Soc.* **1999**, *121*, 2679–2685.
[61] U. Samanta, D. Pal, P. Chakrabarti, *Proteins Struct. Funct. Bioinf.* **2000**, *38*, 288–300.
[62] P. Chakrabarti, R. Bhattacharyya, *Prog. Biophys. Mol. Biol.* **2007**, *95*, 83–137.
[63] O. Guvench, C. L. Brooks III, *J. Am. Chem. Soc.* **2005**, *127*, 4668–4674.
[64] R. Mahalakshmi, S. Raghothama, P. Balaram, *J. Am. Chem. Soc.* **2006**, *128*, 1125–1138.
[65] J. W. Neidigh, R. M. Fesinmeyer, N. H. Andersen, *Nat. Struct. Biol.* **2002**, *9*, 425–430.
[66] TOPSPIN, NMR Data Acquisition and Processing Software, Bruker Biospin, Karlsruhe (Germany).
[67] D. S. Wishart, C. G. Bigam, J. Yao, F. Abildgaard, H. J. Dyson, E. Oldfield, J. L. Markley, B. D. Sykes, *J. Biomol. NMR* **1995**, *6*, 135–140.
[68] K. Wüthrich, *NMR of Proteins and Nucleic Acids*, Wiley, New York, **1986**.
[69] K. Wüthrich, M. Billeter, W. Braun, *J. Mol. Biol.* **1984**, *180*, 715–740.
[70] T. D. Goddard, D. G. Kneller, Sparky 3, NMR Assignment Program, University of California, San Francisco (USA).
[71] P. Güntert, C. Mumenthaler, K. Wüthrich, *J. Mol. Biol.* **1997**, *273*, 283–298.
[72] G. Cornilescu, F. Delaglio, A. Bax, *J. Biomol. NMR* **1999**, *13*, 289–302.
[73] R. Koradi, M. Billeter, K. Wüthrich, *J. Mol. Graph.* **1996**, *14*, 29–32.
[74] N. H. Andersen, J. W. Neidigh, S. M. Harris, G. M. Lee, Z. Liu, H. Tong, *J. Am. Chem. Soc.* **1997**, *119*, 8547–8561.

Received: December 19, 2008

